Dual-Purpose Canister Filling Demonstration Project Progress Report at ORNL, FY 2023

Spent Fuel and Waste Disposition

Prepared for
US Department of Energy
Spent Fuel and Waste Science and Technology
Jeffrey A. Fortner, Eliott J. Fountain, Adrian S. Sabau, and Thomas R. Muth
Oak Ridge National Laboratory

September 29, 2023
M3SF-23OR010305042
ORNL/SPR-2023/3143

This is a technical report that does not take into account contractual limitations or obligations under the Standard Contract for Disposal of Spent Nuclear Fuel and/or High-Level Radioactive Waste (Standard Contract) (10 CFR Part 961). To the extent discussions or recommendations in this report conflict with the provisions of the Standard Contract, the Standard Contract governs the obligations of the parties, and this report in no manner supersedes, overrides, or amends the Standard Contract. This report reflects technical work which could support future decision making by DOE. No inferences should be drawn from this report regarding future actions by DOE, which are limited both by the terms of the Standard Contract and Congressional appropriations for the Department to fulfill its obligations under the Nuclear Waste Policy Act including licensing and construction of a spent nuclear fuel repository.

APPENDIX E
NFCSC DOCUMENT COVER SHEET[1]

Name/Title of Deliverable/Milestone/Revision No. M3SF-23OR010305042

Work Package Title and Number DPC Fillers R&D – ORN SF-23OR01030504

Work Package WBS Number 1.08.01.03.05

Responsible Work Package Manager JeffreyA.Fortner (Name/Signature)

Date Submitted September 29, 2023

Quality Rigor Level for Deliverable/Milestone[2]	☐ QRL-1 ☐ Nuclear Data	☐ QRL-2	☐ QRL-3	☒ QRL-4 Lab QA Program[3]

This deliverable was prepared in accordance with Oak Ridge National Laboratory
(Participant/National Laboratory Name)

QA program which meets the requirements of

☒ DOE Order 414.1 ☐ NQA-1 ☐ Other

This Deliverable was subjected to:

☒ Technical Review ☐ Peer Review

Technical Review (TR)
Review Documentation Provided

☐ Signed TR Report or,

☐ Signed TR Concurrence Sheet or,

Concurrence Sheet or,

☒ Signature of TR Reviewer(s) below

Reviewer(s) below

Peer Review (PR)
Review Documentation Provided

☐ Signed PR Report or,

☐ Signed PR

☐ Signature of PR

Name and Signature of Reviewers

Riley Cumberland (ORNL) Riley Cumberland

NOTE 1: *Appendix E should be filled out and submitted with the deliverable. Or, if the PICS:NE system permits, completely enter all applicable information in the PICS:NE Deliverable Form. The requirement is to ensure that all applicable information is entered either in the PICS:NE system or by using the NFCSC Document Cover Sheet*

- *In some cases there may be a milestone where an item is being fabricated, maintenance is being performed on a facility, or a document is being issued through a formal document control process where it specifically calls out a formal review of the document. In these cases, documentation (e.g., inspection report, maintenance request, work planning package documentation or the documented review of the issued document through the document control process) of the completion of the activity, along with the Document Cover Sheet, is sufficient to demonstrate achieving the milestone.*

NOTE 2: *If QRL 1, 2, or 3 is not assigned, then the QRL 4 box must be checked, and the work is understood to be performed using laboratory QA requirements. This includes any deliverable developed in conformance with the respective National Laboratory / Participant, DOE or NNSA-approved QA Program.*

NOTE 3: *If the lab has an NQA-1 program and the work to be conducted requires an NQA-1 program, then the QRL-1 box must be checked in the work Package and on the Appendix E cover sheet and the work must be performed in accordance with the Lab's NQA-1 program. The QRL-4 box should not be checked.*

This page is intentionally left blank.

SUMMARY

The US DOE Office of Nuclear Energy is investigating the feasibility of direct disposal of dual-purpose canisters (DPCs) in a hypothetical geological repository to offset the potential requirement to repackage spent nuclear fuel (SNF) from existing DPCs into smaller, disposal-ready canisters. Oak Ridge National Laboratory (ORNL) is currently evaluating the feasibility of filling void space in loaded DPCs with an engineered material to prevent a criticality event caused by groundwater/moderator intrusion. Metal alloys are being investigated as a filler material because of their relatively low viscosities when molten, which may facilitate their injection via an existing drainpipe that runs almost the full length of the DPC. ORNL's strategy for evaluating filler viability includes simulations and physical demonstrations of filling and casting behavior, as well as evaluations of materials for compatibility in the repository environment. Filling of DPCs in this manner is expected to mitigate the risk associated with a post-closure criticality event during the repository performance assessment time frame (10,000 years or greater).

Efforts in this fiscal year focused on (1) destructive analysis of experimental filler castings made in FY 2022, (2) a report outlining a conceptual design of a DPC filling facility (Fortner et al., 2023, M3SF-23OR010305044/ ORNL/SPR-2023/2921, May 31, 2023), (3) a report on affected features, events, and processes (FEPs) due to DPC filling (Price et al., 2023, M3SF-23SN010305093, issuance pending), (4) developing and testing a more practical[a] alloy filler based upon a Sn-Al eutectic, and (5) modeling the heating and cooling dynamics of a DPC subjected to molten metal filling. The preliminary results from each of these tasks support the feasibility of filling DPCs with metal as a strategy against the possibility of criticality in the repository. The FY 2022 casting was found to penetrate even very small orifices in the mold and internal structures. Preliminary testing of the Sn-Al eutectic indicate little interaction of the melt with Zircaloy cladding. Thermal modelling shows that a filled DPC will cool to manageable temperatures within 2-3 days, which is likely manageable in a facility.

This report documents work performed supporting the US Department of Energy (DOE) Nuclear Energy Spent Fuel and Waste Disposition, Spent Fuel and Waste Science and Technology, under Work Breakdown Structure element 1.08.01.03.05, "Direct Disposal of Dual Purpose Canisters." In particular, this report fulfills M3 milestone, M3SF-23OR010305042, "DPC filling annual progress report – ORNL," under Work Package SF-23OR01030504, "DPC Fillers R&D – ORNL Annual Progress Report," within Work Package SF-23OR0130505, "DPC Fillers R&D – ORNL."

A separate Activity, SF-22OR10305054, "Develop Acceptance Criteria for Filled Canister," was reported in a previously issued M3 milestone, M3SF-22OR010305054.

[a] More practical in that cost, availability, scalability, durability, materials interactions, and working temperature (i.e., melting point) are favorable for actual field deployment compared with the Bi-Sn eutectic examined in FY 2022.

This page is intentionally left blank.

ACKNOWLEDGMENTS

The authors wish to thank Tim Gunter, Dave Sassani, Geoff Freeze, and Stephanie Booth for supporting this work and Laura Price and Mark Rigali of Sandia National Laboratories for stimulating discussions.

This page is intentionally left blank.

CONTENTS

This page is intentionally left blank.

LIST OF FIGURES

LIST OF TABLES

ACRONYMS

BWR	boiling water reactor
Cp	calculated specific heat
CTE	coefficient of thermal expansion
DOE	US Department of Energy
DPC	dual-purpose canister
DTA	differential thermal analysis
FCRD	Fuel Cycle Research and Development
FEP	Feature, Event, or Process
FY	fiscal year
k	thermal conductivity
LMP	low melting point
LMPA	low-melting-point alloy
MCM	mock-up cask molds
NE	DOE Office of Nuclear Energy
ORNL	Oak Ridge National Laboratory
PWR	pressurized water reactor
SNF	spent nuclear fuel
SNFA	spent nuclear fuel assembly
UNF-ST&DARDS	Used Nuclear Fuel – Storage, Transportation & Disposal Analysis Resource and Data Systems

This page is intentionally left blank.

SPENT FUEL AND WASTE DISPOSITION ORNL DUAL-PURPOSE CANISTER FILLERS R&D ACTIVITIES

1. INTRODUCTION

After spent nuclear fuel (SNF) assemblies are discharged from the reactor and have had sufficient time to cool in wet pool storage, commercial US nuclear utilities typically transfer them to dry cask storage systems that use large dual-purpose canisters (DPCs). Thousands of DPCs that were originally designed for storage and transportation are now loaded with spent fuel and located at independent spent fuel storage installations at reactor sites. These DPCs were not designed to support direct geologic disposal. If directly disposed in a geologic repository, some existing as-loaded DPCs could achieve criticality over the repository performance assessment time frame assuming water (moderator) infiltration and fuel reconfiguration (Hardin et al., 2014; Clarity et al., 2017). Three approaches are under investigation to mitigate this potential for post-closure criticality. The first approach is to perform detailed modeling and analysis of each loaded DPC; this effort is underway using the Used Nuclear Fuel – Storage, Transportation & Disposal Analysis Resource and Data System (UNF-ST&DARDS) (Clarity et al., 2017) to highlight which DPCs are of particular concern. The second approach includes a criticality consequence analysis to determine the impact of a potential criticality event on a repository performance assessment. The third approach is to investigate preconditioning of DPCs with engineering filler materials that can be credited over a repository time frame to displace the moderator material, such as groundwater, needed to achieve in-canister criticality. This report presents the progress made at Oak Ridge National laboratory (ORNL) toward addressing this third approach to support adding a filler material to existing DPCs before placing them into a repository.

Repackaging the fuel assemblies from these DPCs into smaller, disposal-ready canisters would entail significant expenses, waste, and risks. One potential method to significantly reduce the risk that water ingress could initiate criticality within a DPC is to backfill DPCs with a remedial material that fills void space. To establish confidence in this mitigation function, the filler material must be put in the DPCs without significant voids or defect volume. It must also not cause significant damage to the entrained SNF assemblies, or to the DPC itself. The DOE Office of Nuclear Energy (NE) is currently investigating the feasibility of direct disposal of DPCs in a geological repository to potentially offset the need to repackage SNF currently loaded in DPCs into smaller disposal canisters and is therefore supporting the investigation of some candidate filler materials.

DPCs presently accommodate up to 37 pressurized water reactor (PWR) assemblies and 89 boiling water reactor (BWR) assemblies, and they are designed primarily for storage and transportation (hence “dual purpose”). DPC direct disposal has many potential benefits, including cost savings on the order of billions of dollars, minimization of potential incidents and worker dose incurred from repackaging activities, and the elimination of low-level radioactive waste in the form of discarded DPCs (Cumberland et al., 2022). Although it has been indicated that direct disposal of filled DPCs is feasible from a purely technical perspective (Cumberland et al., 2022), several engineering challenges as well as legal and policy issues must be addressed to make DPC disposal a reality. The technical challenges include demonstrating the practicality of fillers to mitigate against potential post-closure criticality in a repository and demonstrating that DPCs can be filled reliably and economically for this purpose.

2. EXAMINATION OF FY 22 FILLING AND SOLIDIFICATION EXPERIMENTS

In FY 2022, two demonstration experiments were conducted. This effort was a significant scale-up of a metal casting relevant to DPC filling. The mock-up cask molds (MCM), which contained several sections specific to DPCs (Figure 1a), were initially filled with molten eutectic Sn-Bi alloy. The FY 22 internal mock-up test assembly shown in Figure 1a included a 5 × 5 array of simulated fuel rods on top of a stand that represented the bottom spacer (Fortner et al., 2022). The stainless steel rods simulated the size and spacing of fuel rods in a PWR assembly. The poured Sn-Bi eutectic alloy solidified in the MCM (Figure 1b), as described in last year's report. Destructive analysis of the Sn-Bi castings was conducted in FY 23.

An image of a cross-sectioned Sn-Bi casting is shown in Figure 2. This part of the casting was cut through the mockup fuel-rod region in both the horizontal and vertical directions. This cross-sectional image shows a complete infiltration of the Sn-Bi eutectic through the mock-up fuel rods. Another image of the cross-sectioned Sn-Bi casting through the fuel-rod and bottom spacer regions is shown in Figure 3. An image similar to that shown in Figure 2 is Figure 4 after the stainless steel rods were removed. It should be noted that the circle, which appears in the lower left-hand corner of the casting in Figure 4, is the filler steel tube, through which the metal was poured. The stainless steel rods were mechanically punched out. The mechanical removal of the rods is thought to have minimally affected the surface condition of the casting holes as significant adhesion of the eutectic to the metal rods. The central hole (top surface in Figure 4) included the coupling to the central stand between the rods and the bottom spacer (central region of Figure 1a), which was left partially intact during the rod removal. In fact, a thin foil of eutectic infiltrated the narrow space between the central rod and the stand and is visibly flaking, as shown in Figure 4. Both horizonal and vertical surfaces shown indicate that there were no surface defects, cracks, or voids. An examination of internal surfaces revealed that the wetting between the rods and the Sn-Bi alloy was excellent. In conclusion, the visual inspection showed that (a) all of the interstitial spaces within the simulated fuel and other internal features were adequately filled, (b) there were no obvious voids or cracks, and (c) wetting of the rods by the molten Sn-Bi alloy was excellent.

These very good results prompted FY 23 efforts to focus on exploring practical, "deployable" alloy fillers and interaction tests with Zircaloy rather than a scale-up of the filling and casting demonstration. A scale-up experiment using a deployable alloy is envisioned for FY 24.

(a) (b)

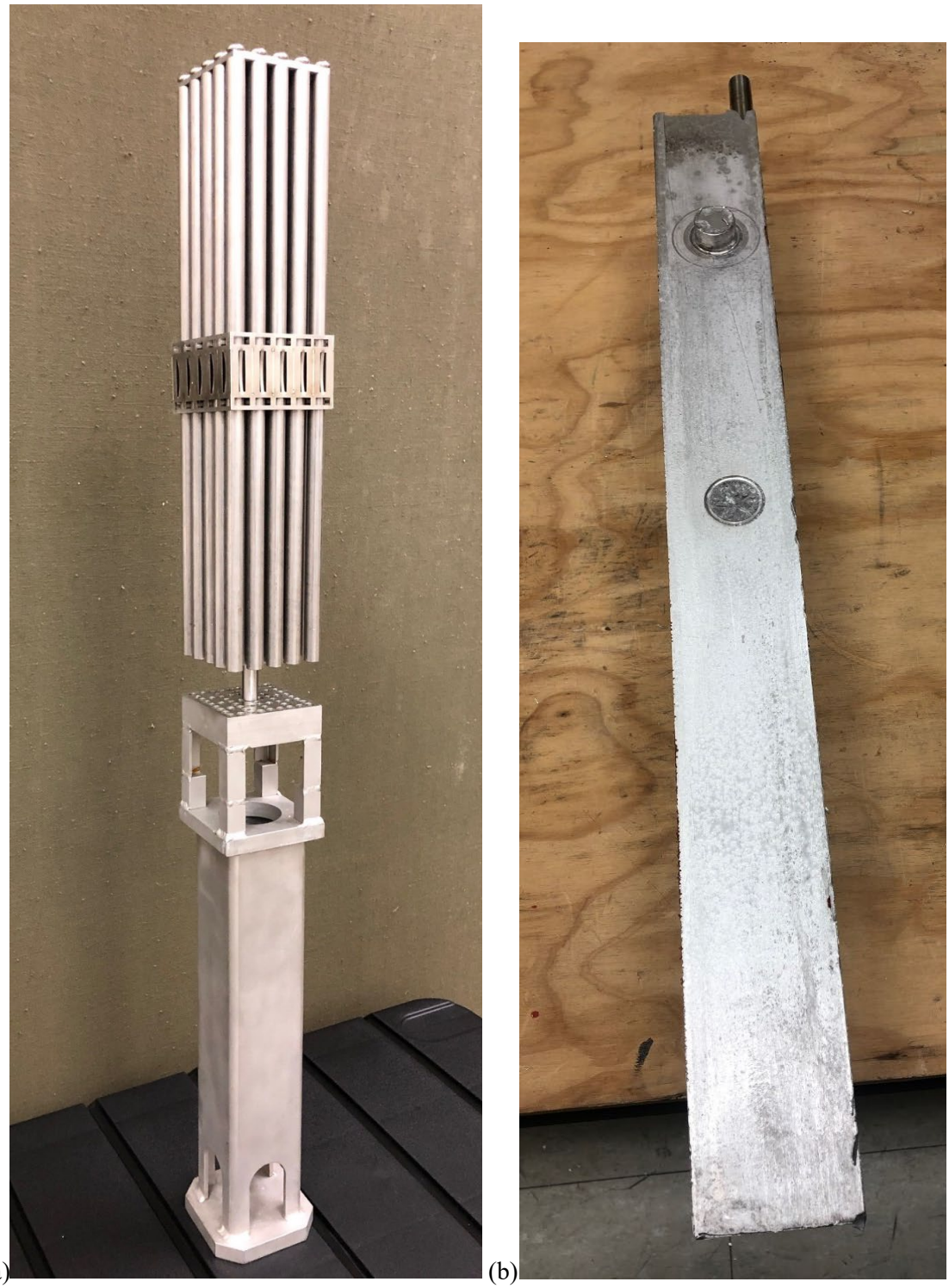

Figure 1. DPC mock-up experiments: (a) FY 22 internal mock-up test assembly without the filler tube, (b) Sn-Bi casting with the filler tube (Fortner et al., 2022).

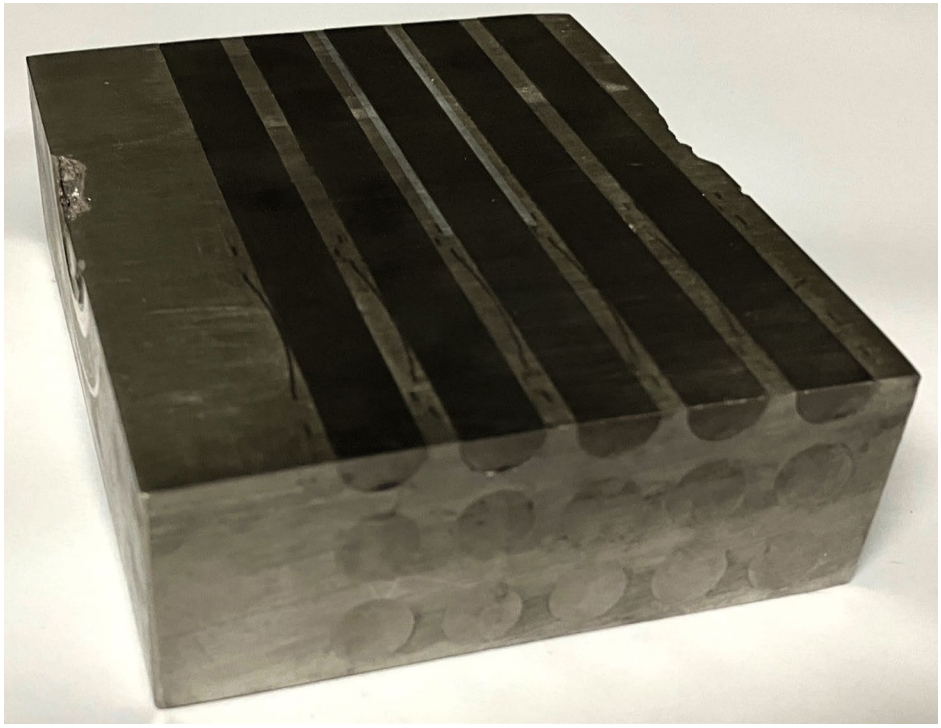

Figure 2. Image of a Sn-Bi casting and stainless steel rods cross-sectioned in the vertical and horizontal directions through the rod spacer grid region.

(a)

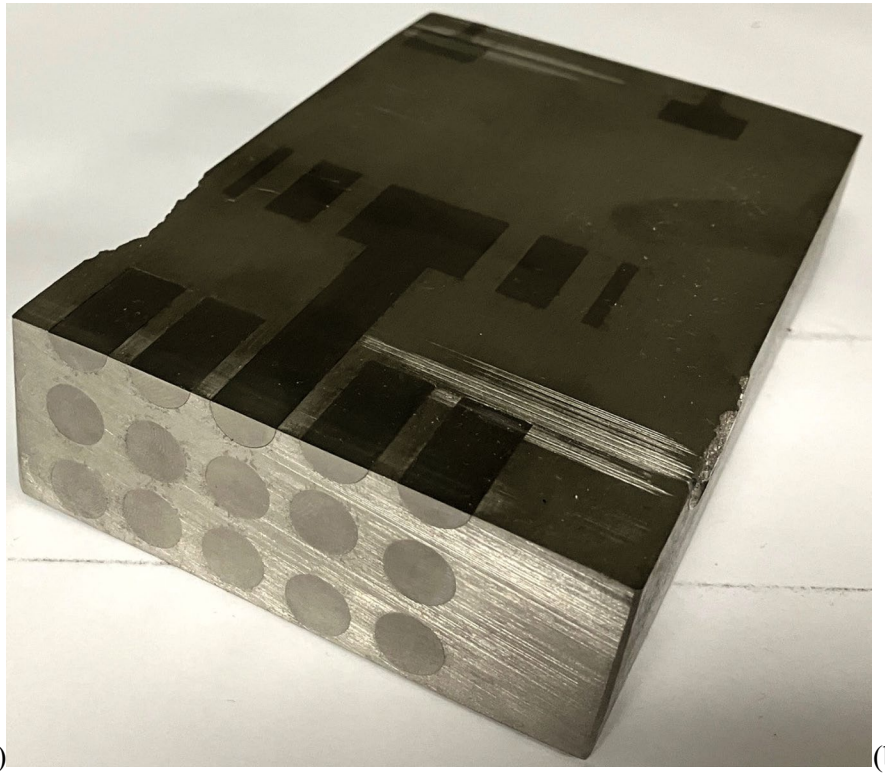

(b)

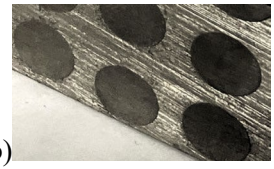

Figure 3. Image of a Sn-Bi casting and stainless steel rods cross-sectioned in the vertical and horizontal directions through the fuel-rod and bottom spacer regions: (a) entire section, (b) inset of the horizontal cross section with enhanced contrast.

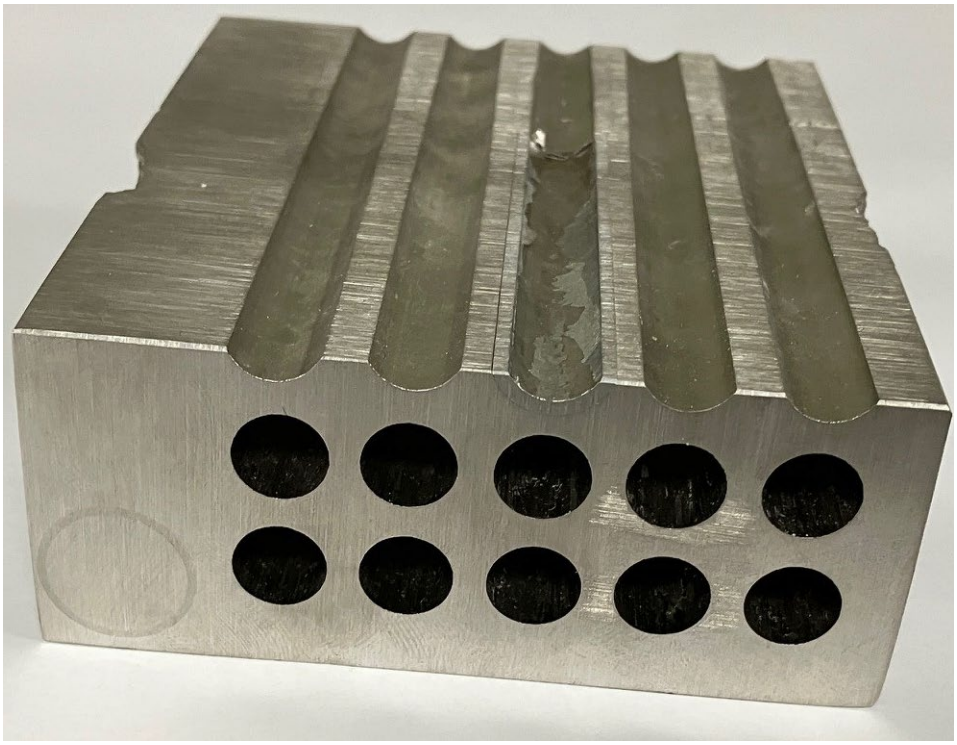

Figure 4. Image of a Sn-Bi casting cross-sectioned in vertical and horizontal directions through the fuel-rod region (stainless steel rods removed).

3. REVIEW OF Zn-Al MATERIALS COMPATIBILITY WITH ZIRCALOY

One of the main requirements for using metallic fillers for DPC is appropriate material compatibility with Zircaloy. No study was found specifically on Zn-Al eutectic melt compatibility with Zircaloy, but there has been some interest in the reaction between zinc and zirconium/Zircaloy at high temperature (Williams et al., 2000; Schaefer et al., 2000) and even in PWR cooling water (Gold et al., 1996). For purposes of a DPC filler, we would argue that some interaction is acceptable, provided there is no danger of through penetration direct interaction with the fuel pellets and that the alloy suitably fills the void spaces. A filled DPC will no longer be relying on the cladding to provide any mechanical structure, and most performance assessments have not credited the cladding as being a barrier (DOE, 2004). The remainder of this section will summarize a literature review of Al alloy and Zircaloy compatibility.

Zn-Al alloys have been used for several applications, such as for die casting application and soldering at high temperature, and were found to exhibit excellent castability (Türk et al., 2007). To improve the quality and performance die castings, Zn-Al alloys were developed, such as AG-40A, AC-41A, and AC-43A alloy (ASTM). ZnAl4 alloy (AG-40A) is the most used general-purpose Zn die casting alloy. As the addition of Zr to Al-based alloys was beneficial to microstructure and material properties, and as the primary phase of Zn-Al alloys is an Al-rich solid solution, it is expected that Zr (element) in Zn-Al alloys will have similar effects to that in Al alloys. Indeed, the effect of Zr addition (0.05 to 0.3 % wt.) in ZnAl4 alloy was shown to have a similar beneficial effect to that for Al alloy (Li et al., 2014).

A review of low-melting-point alloys (LMPAs) needs to be conducted to identify metallic alloys with low melting points for the DPC filling application. Some requirements for fillers to be used in DPC filling applications were formulated in several studies (Jubin et al., 2015; Maheras et al., 2012; Puig et al., 2008). The DPC and fuel rods assemblies act as a permanent mold[†], to use the metal casting terminology. On

[†] *permanent mold* refers to a metal mold

the other hand, the slow cooling rate, which would be experienced by the alloy in the filled DPC, would be those typical for the sand casting process. Thus, in addition to the requirements for nuclear fuel considerations, other requirements can be adapted from those related to metal casting. For example, a low solidification interval‡ in the same alloy family was shown to reduce shrinkage defects, such as voids and cracking, during casting solidification. Moreover, a larger solidification shrinkage, which is defined as the linear or volumetric change during solidification, would aggravate casting defects.

Low-melting point alloys were developed for quite a few applications, including solder materials (Dobosz and Gancarz, 2018), brazing (Peng et al., 2021), latent heat energy storage for thermal energy storage (Risueño et al., 2017), galvanized coating applications (Chen and Willis, 2005), and die casting (ASTM, 2022; Barnhurst, 1990). In fact, some of the LMPAs were developed solely for each of the niche applications identified above. Zn-containing alloys were selected as DPC filler candidates mainly due to their low melting points. The literature review indicated that only selected material properties, which are critical for the original low-melting-point application, were measured. Thus, some material properties that are required for DPC fill screening are needed. In addition to materials selection, material properties of metallic alloys are needed for the numerical simulation of defect formation during DPC filling. This report also presents the material properties of several LMPAs, such as Zn-Al eutectic and Zn-4Al-3Mg alloy.

3.1 Review of Commercial Zn-Al Alloys

Zinc alloys have been used for die casting since the 1920s (Barnhurst, 1990). Until the 1970s, all Zn alloys were based on a hypoeutectic composition, containing less aluminum (~4% Al) than the eutectic chemistry of 5.0% Al. Since the 1970s, a family of hypereutectic Zn-Al alloys (>5% Al) has become widely used as die casting alloys. The hypoeutectic and hypereutectic Zn-Al alloys are referred to as Zamak and ZA alloys (Barnhurst, 1990), respectively (Table 1). Zamak has been chosen as the common name to define all Zn alloys for the die casting process.

Zinc alloys have low melting points, require relatively low heat input, do not require fluxing or protective atmospheres, and are nonpolluting. The composition, density at room temperature, solidus temperature (T_S), liquidus temperature (T_L), latent heat of fusion (dH), and recommended pouring temperature (T_{Pour}) are given in Table 1 (Barnhurst, 1990). No published reference for latent heat for Zamak alloys was found. The recommended casting temperature is also listed. Additional properties that are relevant to the DPC filling/solidification application of ZA and Zamak Zn-Al alloys are given in Table 2. Due to their high fluidity, Zn alloys can be cast in much thinner walls (as low as 0.13–0.75mm) than other die castings alloys (Goodwin, 2013; Pola et al., 2010), which is a very good characteristic for the DPC filling application. Some of Zn-Al alloys have been modified by the addition of elements, e.g., Mg (Chen et al., 2003), to improve their mechanical, tribological, and corrosion resistance properties.

‡ *solidification interval* indicates the temperature range between the liquidus temperature and solidus temperature.

Table 1. Composition, trade names, and main properties of ZA and Zamak Zn-Al alloys.

Composition (% wt.) and trade name(s)	ρ @RT [g/cm^3]	T_S [°C]	T_L [°C]	dH [kJ/kg]	T_{Pour} [°C]
Zn-8Al-1Cu-0.02Mg (ZA8)	6.3	375	404	112	435–460
Zn-11Al-1Cu-0.025Mg (ZA12)	6.03	377	432	118	460–490
Zn-27Al-2Cu-0.015Mg (ZA27)	5	376	484	128	515–545
Zn-4Al-0.04Mg (AG40A, Zamak-3)	6.6	381	387		395–425
Zn-4Al-2.5Cu-0.04Mg (AC43A, Zamak-2)	6.6	379	390		395–425
Zn-4Al-1Cu-0.05Mg (AC41A, Zamak-5)	6.7	380	386		395–425
Zn-4Al-0.015Mg (AG40B, Zamak-7)	6.7	381	387		395–425

References for the material property data shown in Table 2 are as follow.

a) Linear solidification shrinkage $d\varepsilon_{L-S}$ (Barnhurst, 1990). Although the $d\varepsilon_{L-S}$ data from Barnhurst (1990) is given as "Volume change on freezing," the public data distributed with the metal casting software ProCAST for Zamak-2, Zamak-3, and Zamak-5 indicate that that the $d\varepsilon_{L-S}$ data (Barnhurst, 1990) is actually the "linear" and not the "volumetric" change on freezing. This needs to be further confirmed with experimental data (Liu, 2006).

b) Thermal conductivity, k, at room temperature (Barnhurst, 1990). Thermal conductivity is important for the DCP as the fuel-generated heat must be dissipated.

c) Viscosity at the liquidus temperature, μ_L, of Zamak alloys from public data distributed with ProCAST software. μ_L of ZA alloys from Eqal and Yagoob (2021). The viscosity is one variable that can be used to infer the fluidity during castings.

The following considerations have to be taken into account for casting of Zn-Al alloys (Barnhurst, 1990).

a) Strict adherence to chemical composition limits and proper die design are necessary to minimize casting defects and attain high strength and ductility.
b) Impurities content has to be within the ASTM B86 limits. For die cast components, exceeding the impurity limits can result in intergranular corrosive attacks and premature failures by warping and cracking.
c) For all Zn-Al alloys (excluding Zamak-7), high melting/pouring temperatures should be avoided to prevent Mg loss. Alternatively, Mg content can be adjusted based on holding times and melting temperatures.
d) Zn-Al alloy melts must be stirred well, allowing a 15 min holding period. The surface dross must be skimmed.
e) For all Zn-Al alloys, microstructural changes with time can alter the properties and dimensions of cast parts. However, due to slow cooling rates for the DPC filler application, which we estimate to be lower than those for sand castings, the dimensional stability, which must be addressed for typical Zn die castings due to high cooling rates, is not a concern.
f) Large castings of ZA27 are prone to underside shrinkage, which is caused by gravity segregation of the Al-rich phase during solidification and subsequent roughening on the drag surface of the casting as Zn liquid feeds the solidification shrinkage into the casting.

Table 2. Additional material properties of ZA and Zamak Zn-Al alloys.

Alloy	$d\varepsilon_{L-S}$ [%]	k [W/m-K]	μ_L (mPa s)	Castability, uses, characteristics
ZA8	1	115	2.9	Casting in ferrous permanent molds, gravity casting
ZA12	1.3	116	2.7	Gravity casting, pressure die casting
ZA27	1.3	126	2.1	Sand casting (optimum)
Zamak-3	1.17	113	2	Excellent castability; long-term dimensional stability
Zamak-2	1.25	105	4.1	Gravity casting, sand casting With aging it becomes more brittle, shrinks more
Zamak-5	1.17	109	3.4	Higher corrosion resistance than Zamak-3 but reduced ductility and dimensional accuracy
Zamak-7	1.17	109		Higher inter-granular corrosion resistance, more fluidity than Zamak-3, better for thin wall castings

Zamak-3 was considered to fill externally accessible void spaces inside a disposal package containing a spent nuclear fuel assembly (SNFA) to increase the effective thermal conductivity of the package such that the heat transfer mechanisms would be dominated by conduction (Park et al., 2017).

3.2 Review of Low-Melting-Point Filler Candidates

Aside from the Zn-Al alloys, few LMPAs, which were included in several Zn-Al studies for comparison purposes, were included in this study. In this literature review, Ge, Ga, In, and Li alloying elements were excluded due to their rarity or high cost. Pb was also excluded from review.

For alloy screening purposes, the following properties are considered: density ρ at room temperature, dynamic viscosity μ_L at the liquidus temperature, liquidus temperature T_L, solidus temperature T_S, latent heat of fusion, and linear solidification shrinkage. The eutectic reaction is isothermal, i.e., $T_L = T_S$ for eutectic alloys. The addition of Cu was found to enhance the creep properties in Zn–3Cu–xAl alloys (Alibabaie and Mahmudi, 2012).

The very-low-melting-point Al alloys were also included in the review. Al alloys with low melting points were originally developed for brazing applications (Chuang et al., 2000; Peng et al., 2021). By adding 1, 1.5, and 2 wt.% Ni to the ternary Al-6.5Si-20Cu wt.% alloy, the T_S and T_L temperatures changed within 1°C and 2°C, respectively (Peng et al., 2021). The T_S and T_L of these Al-Si-Cu-Ni alloys, which were measured using differential thermal analysis (DTA), were found to be 519.8~528.4°C, 520.8~528.2°C, and 519.2~526.8°C, respectively. Two Al-Si-Cu-Zn alloys with T_L temperatures below 500°C, which were selected from the 14 alloys investigated for brazing applications (Tsao et al., 2002), are shown in Table 3. Material properties, which were experimentally measured, are shown in Table 3 for the alloys considered. For the sake of completion, eutectic SnCu and SnZn binary alloys are also shown in Table 3. For convenience, the atomic compositions of main alloys considered are given in Table 7.

Table 3. Experimentally determined properties of eutectic alloys Zn-Al, Zn-Al-Mg, Zn-Mg, Sn-Cu, Sn-Zn, including very low melting point Al alloys.

Composition (% wt.)	ρ [g/cm^3]	T_S [°C]	T_L [°C]	dH [kJ/kg]	$d\varepsilon_{L-S}$ [%]	k [W/m-K]	T_{Pour} [°C]	Ref.
Zn-5Al	6	381	381	118	1.28	134	400–420	a, b
Zn-4Al-3Mg	6.19	344	344	133	1.28	70	360–390	b
Zn-3.7Al-2.4Mg	6.19	344	344	104	1.3	59	360–380	c
Zn-7.05Al-3.85Cu		372	372				390–410	h
Zn-6Al-1Cu		371	375				390–410	i
Zn-6Al-2Cu		370	380				395–415	i
Zn-6Al-3Cu		370	384				400–420	i
Zn-4Al-3Cu-1Mg		335	377				390–410	j
Zn-0.25Cu-0.4Ni		415	439				460–480	g
Mg-47Zn-3.9Al	2.82	340	340	157	1.17	47	350–370	c
Al-6.5Si-20Cu		519.2	526.8				560–580	d
Al-7Si-20Cu-2Sn-1Mg		501	522				560–580	e
Al-7.2Si-20Cu-20Zn		456	496				530–550	f
Al-6Si-20Cu-30Zn		429	482				520–540	f
Sn-9Zn	8.8	227	227				250–270	a
Sn-8.8Zn	6.98	200	200				220–240	a

References are indicated as follows: a (Dobosz and Gancarz, 2018), b (Risueño et al., 2017), *c* (Risueño et al., 2015), d (Peng et al., 2021), e (Chuang et al., 2000), f (Tsao et al., 2002), g (M. M. Hasan et al., 2020a), h (Petzow, 1991), i (Kim et al., 2008), j (da Costa et al., 2009)

Pouring temperatures, T_{Pour}, were estimated by assuming similar superheat temperatures (T_{Pour} - T_L) as those for commercial Zn-Al alloys (Table 1). The fields for the data, which was not measured experimentally, were left unfilled. Thus, there is limited information about the material properties of these alloys that is needed for their initial screening or numerical simulations needed to evaluate their use in DPC application.

Other material properties needed to fully evaluate these candidate materials for the DPC filler application can be obtained from thermodynamic simulations (Chen and Zhang, 2020; Liang et al., 2019). Unless indicated, the material properties listed in Table 4 were obtained with Al or Mg databases from the thermodynamic CALPHAD Pandat software. By comparing the data for experimentally determined Ts and T_L (Table 3) with those computed from Pandat using Al and or Mg databases (Table 4), it can be seen that, with the exception of Al-Si-Cu alloys, the T_L and T_S temperatures were predicted quite accurately. The predicted solidification shrinkage was almost 40–60% greater than those experimentally measured for zinc-dominant alloys. Thus, appropriate databases, which were validated for Zn alloys, must be used to accurately predict material properties (Liang et al., 2019).

Table 4. Computed properties of selected low melting point alloys.

Composition (% wt.)	ρ [g/cm^3]	T_S [°C]	T_L [°C]	dH [kJ/kg]	$d\varepsilon_{L-S}$ [%]	k [W/m-K]	μ_L (mPa s)
Zn-5Al	6.9	382	382	126.8	2.15	102	4.1
Zn-4Al-3Mg	6.4	345	354	137.8	1.95	75	4.6
Zn-3.7Al-2.4Mg	6.512	345	345	128.4	1.94	80	4.9
Zn-4.3Al-0.6Cu-0.31Mg*		344	382				
Zn-4Al-3Cu-1Mg*		344	368				
Mg-47Zn-3.9Al	3.17	336	336	178.4	5.26	67	6.6
Al-6.5Si-20Cu	3.31	523	627		2.82	130	2
Al-7Si-20Cu-2Sn-1Mg	3.25	478	532	461.5	2.42		2.1

* (Liang et al., 2019)

3.3 Material Properties of Zn-Al Binary Eutectic and Zn-4Al-3Mg

The microstructure model in ProCAST (Guo and Samonds, 2007, 2004), which also includes Al material database and PANDAT thermodynamic solvers (Cao et al., 2009), was used to conduct thermodynamic simulations for the alloys considered based on the Lever rule model. The Lever rule assumption was selected based on the low cooling rates expected. For the binary eutectic, Zn-5Al, calculated specific heat (Cp), thermal conductivity (k), and coefficient of thermal expansion (CTE) are shown in Figure 5. The specific heat was calculated from the thermodynamic enthalpy data. The thermophysical properties shown in Figure 5 exhibit discontinuities due to the eutectoid phase transformation of unstable γ phase to lamellar α + η phase at 275°C.

For the Zn-5Al alloy, Cp was calculated as 0.309J/(g·K) from the graph of heat flow vs. temperature (Engin et al., 2011). This is in reasonable agreement with data shown in Figure 5a. Typically for metals, the thermal conductivity in the liquid phase is almost a half of that of the solid phase.

For the Zn-5Al alloy, the mean CTE over a temperature range of 30–270°C was estimated to be 4.74e-5 [1/K], while the mean CTE estimated over the same temperature range from thermal mechanical analysis data was CTE = 3.22e-5 [1/K] (Hasan et al., 2020b). Thermodynamic modes for the Zn-Al-Cu-Mg quaternary alloy system were developed by Liang et al. (2019) and show good agreement with experimentally measured solidification properties.

For the Zn-4Al-3Mg alloy, Cp, k, and CTE are shown in Figure 6. The most notable difference between these properties for the Zn-4Al-3Mg alloy and Zn-5Al alloy is seen in the thermal conductivity (~20% decrease in the solid phase k).

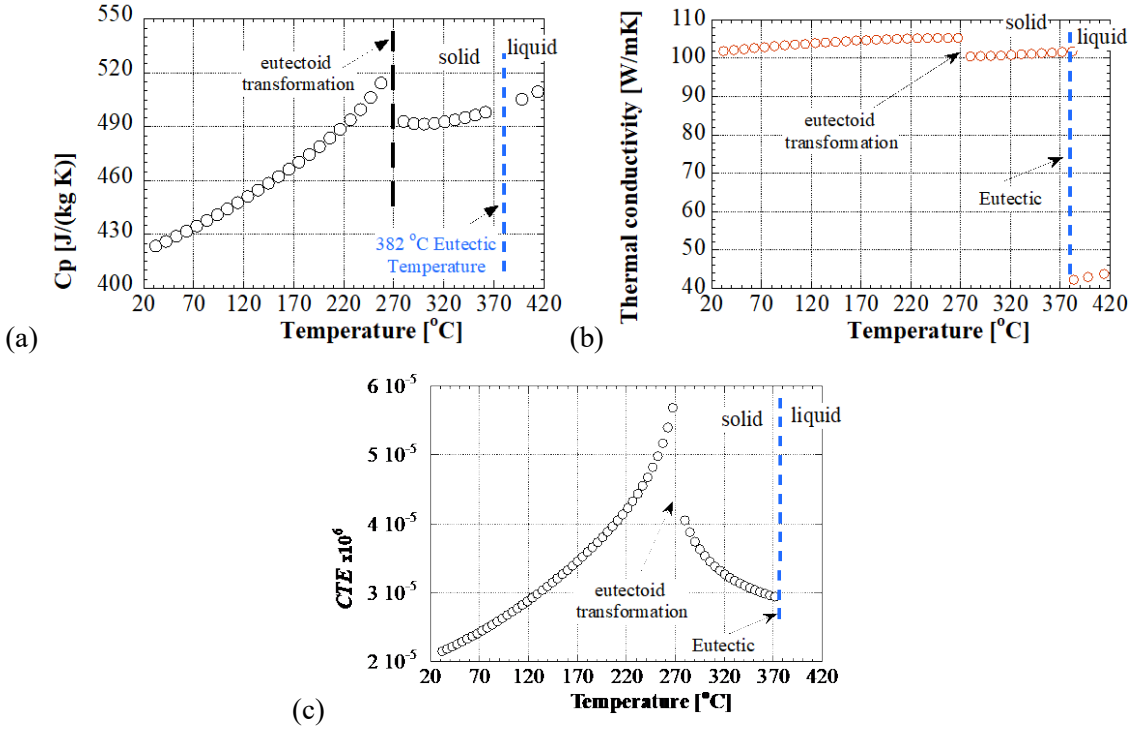

Figure 5. Computed properties for Zn-5Al eutectic binary alloy: (a) specific heat, (b) thermal conductivity, and (c) linear coefficient of thermal expansion.

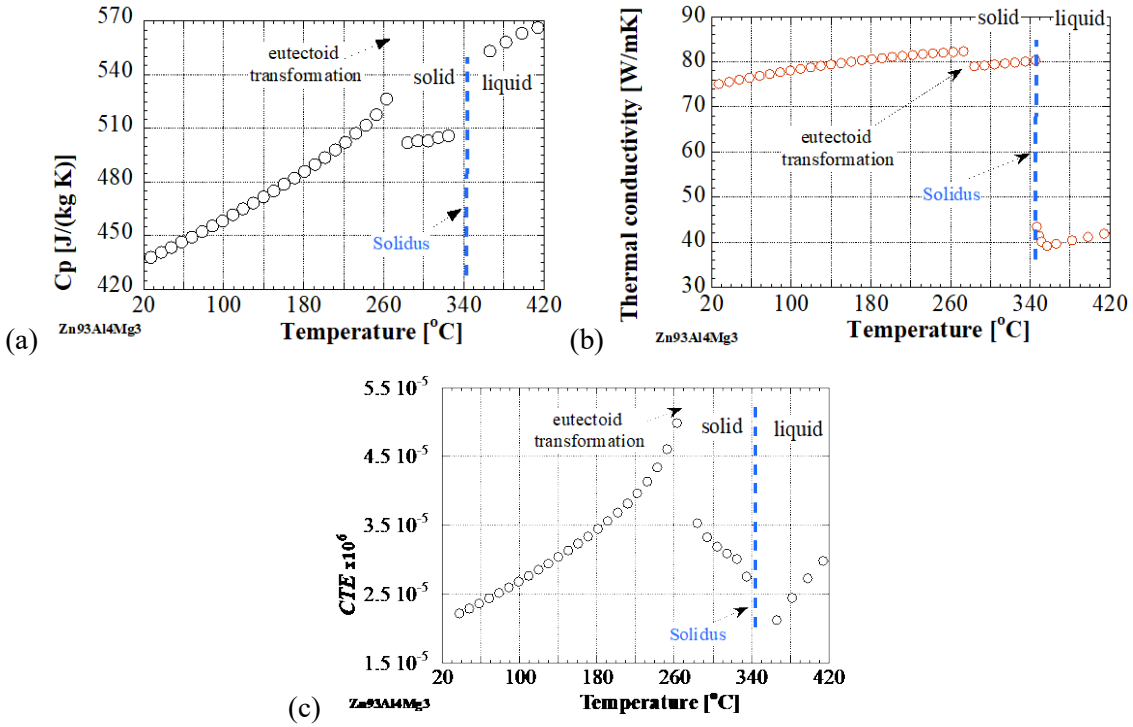

Figure 6. Computed properties for Zn-4Al-3Mg ternary alloy: (a) specific heat, (b) thermal conductivity, and (c) linear coefficient of thermal expansion.

3.4 DPC Heating Temperatures and Pouring Temperatures for Selected Alloys

Based on metal casting experience for Zn alloys, the pouring alloy temperature was between [T_L+50:T_L+100]. Note that the recommended pouring temperature (T_{Pour}) was about [T_L+15:T_L+45] for the Zn-Al alloys (Barnhurst, 1990). The cooling rates for the traditional Al casting processes were obtained from ASM handbooks (Sadayappan and Elsayed, 2018; Sigworth, 2018).

The DPC canister and fuel rods assemblies act as a permanent mold, to use the metal casting terminology. At this preliminary stage in alloy selection, we envisioned the DPC preheating temperature, T_M, to be higher than the T_S but lower than the T_L+20. A narrower range for the T_M can be identified by considering the fill rate and local conditions (temperature, pressure) for filling the narrow passages within the DPC. As shown Table 5, the preheating temperature, T_M, of the DPC filling application is much higher than those of any traditional casting processes. Due to this high mold temperature, we expect that cooling rates for DPC filling application to be smaller than those for the permanent mold casting. Moreover, as the DPC dimensions are quite large, preliminary considerations indicated that cooling rates for the DPC filling application would be those typical of sand casting. Thus, the DPC filling application cannot be classified as one of the typical metal casting processes as it resembles that of a permanent mold casting with the slow cooling typically seen in sand castings.

Table 5. Preheat temperature and cooling rates for traditional casting processes and DPC filling application.

Process	T_M range [°C]	Thin sections Cooling rate range [°C/s]	Large sections Cooling rate range [°C/s]
Sand casting	Room temp.	0.05–5	0.1–0.5
Permanent mold casting	150–200	2–10	0.3–1
Low-pressure die casting	150–300	1–100	0.5–2
DPC filling	T_S – T_L+20	Sand casting (estimate)	Sand casting (estimate)

From the 23 alloys considered, eight alloys in Table 6 were selected based on their low melting points, solidification temperature interval, and recommended T_{Pour}. To further aid in the screening of metallic alloys, the average pouring temperature (T_{Pour}) and the average DPC preheating temperature (T_M) are shown in Table 6. The range is specified as T_{Pour}–dT_{Pour} to T_{Pour}+dT_{Pour}. Similarly, the DPC preheating temperature range is given as T_M–dT_M to T_M+dT_M. The average pouring temperature and DPC preheat temperature (370°C and 355°C, respectively) were found to be for the ternary Zn-4Al-3Mg alloy. The lowest processing temperature was obtained for the quaternary alloy Zn-4Al-3Cu-1Mg (T_{Pour}=385°C and T_M=370°C). Zamak alloys were valid commercially available options with T_{Pour}~410°C and T_M~400°C. The atomic compositions of selected alloys considered are given Table 7.

Table 6. Recommended DPC temperature and pouring alloy temperatures for selected alloys.

Composition (% wt.) and trade name(s)	T_S [°C]	T_L [°C]	T_{Pour} [°C]	$+/-dT_{Pour}$ [°C]	T_M [°C]	$+/-dT_M$ [°C]
Zn-4Al-3Mg	344	344	370	10	355	10
Zn-6Al-1Cu	371	375	400	15	385	10
Zn-4Al-3Cu-1Mg	335	377	385	35	370	35
Zn-4Al-0.04Mg (Zamak-3)	381	387	410	15	400	15
Zn-4Al-2.5Cu-0.04Mg (Zamak-2)	379	390	410	20	395	15
Zn-4Al-1Cu-0.05Mg (Zamak-5)	380	386	410	15	395	15
Zn-4Al-0.015Mg (Zamak-7)	381	387	410	15	400	15
Al-6Si-20Cu-30Zn	429	482	485	40	470	40

Table 7. Atomic and weight composition for main DPC alloy filler candidates, including Zn-Al, Al, and Sn alloys.

Composition (% at.)	Composition (% wt.)
Zn88.7Al11.3	Zn-5Al
Zn84Al8.7Mg7.3	Zn-4Al-3Mg
Zn85.8Al8.2Mg6	Zn-3.7Al-2.4Mg
Mg70Zn24.9Al5.1	Mg-47Zn-3.9Al
Al84.7Si7.2Cu9.8	Al-6.5Si-20Cu
Al80.7Si7.7Cu9.8Sn0.52Mg1.3	Al-7Si-20Cu-2Sn-1Mg
Sn98.2Cu1.8	Sn-9Zn
Sn84.7Zn15.2	Sn-8.8Zn

4. ALLOY DEVELOPMENT AND COMPATIBILITY

A small prototypical casting was proposed that mimics all the relevant geometrical DPC features and materials expected in the fuel rod assemblies. However, before prototypical casting would be made, the potential Zn-Al eutectic metallurgical reaction with Zircaloy-clad uranium oxide fuel elements, which can yield unfavorable $ZrAl_3$ and /or $Zn_{22}Zr$, must be understood. While the casting temperatures are quite low for both reactions to take place, in the full-size process of filling a DPC, the Zn-Al eutectic could stay liquid for days due to the size of the casting. To address the metallurgical reaction concerns, two experiments are planned: one using new Zircaloy 4 tubing and the second using Zircaloy 4 tubing that has been oxidized, to replicate the actual surface condition that is expected in fuel elements currently in dry cask storage and slated for geologic disposal. There is a high probability that the oxidized (actual) Zircaloy may not be wetted by the Zn-Al eutectic, and the concern for creating a reaction can be eliminated. The rationale for conducting experiments on both the new Zircaloy tubing and its oxidized version is to obtain data on a conservative estimate on possible metallurgical reactions (fresh Zircaloy) and a more representative case for the oxidized cladding. If we find no interaction on either new or oxidized Zircaloy, then the next technical challenges pertaining to void filling, solidification defects (voids, cracking), and cooling stresses in the DPC would be addressed.

A master melt of the Zn-Al eutectic was prepared in a small electric Nabertherm furnace (Figures 7 and 8). The crucible can hold approximately 12 kg of alloy (Zn-5 wt% Al density 6.9g/cm3). The alloy melt was created from inventory metals, and a cast of roughly 1 kg of the 12 kg melt into ingots of ~18 mm diameter. The remaining 11 kg was saved for future casting work.

The 18 mm diameter logs were sectioned into 2.5 cm long pieces to fit into small magnesium oxide (MgO) refractory crucibles. These small MgO crucibles contained about 45 g of alloy and were used to conduct the interaction study of the Zircaloy with the molten alloy.

The new Zircaloy 4 tubing was cut into eight short segments ~15 mm long. Four segments were planned for the "new" Zircaloy interaction study, and the other four will be sent to the corrosion group for steam oxidation for later study simulating aged fuel surfaces.

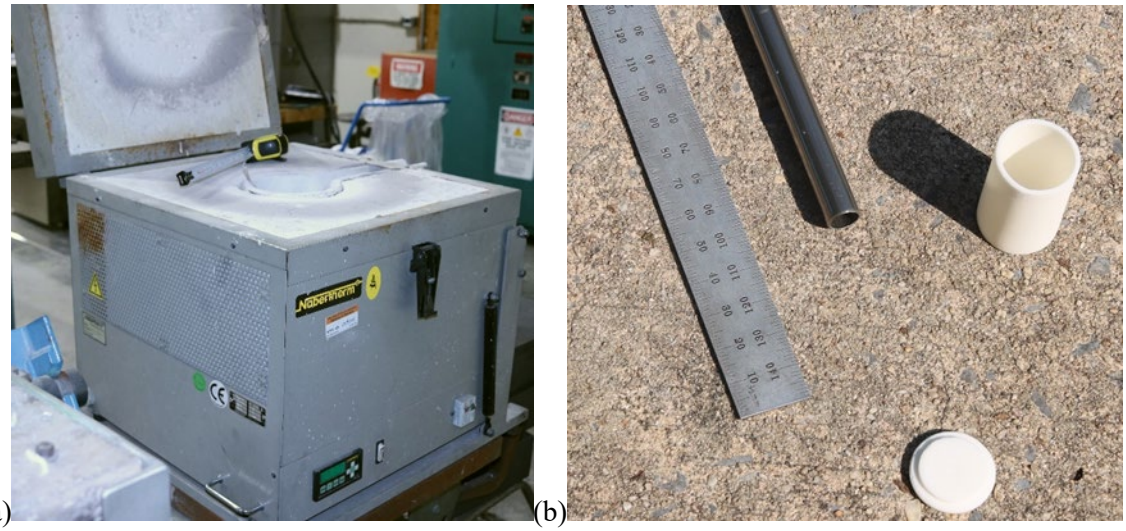

Figure 7. Experimental setup: (a) Nabertherm furnace at the ORNL foundry lab and (b) MgO crucible with fresh Zircaloy tubing.

A single melt of ~1 kg master alloy was produced using pure Zn and Al pellets. Getting the Al to wet the Zn was difficult, so the Zn and Al metals were heated in separate crucibles to 680°C and then the melts were combined into a single crucible. That "master melt" was further divided into three small crucibles, each filled to nearly overflowing. A segment of Zircaloy tubing was cut at a length of approximately ½ in. and submerged into one of the small crucibles. The filled crucible was held for 2 h at a temperature of 400°C. The crucible was removed from the furnace, and the contents were allowed to solidify. The solidified "nugget" was removed by breaking the crucible. A band saw cut of the nugget revealed a large void inside the tube. The large void is likely due to the solidification shrinkage of the last region to solidify. Moreover, the large void could also be due to the entrapped air during filling. Indeed, the tube rotated to the horizontal position during the test, although it was inserted into the molten alloy in the vertical position, i.e., along its axis orientation. Preliminary cross-section light microscopy is shown in Figures 9–11. The study of the Zircaloy-Zn4Al interface was not completed, and only preliminary information was obtained. Examination of preliminary micrographs indicated that minimal signs of a liquid Zn4Al alloy interaction were observed. While it appears that Zircaloy was thinning in some places (Figures 10 and 11), this appearance is likely due to the cross section being made at an oblique angle through the end of the Zircaloy tube section. Based on our literature review for Al-Zr reactions, this thinning after only a 2 h exposure at 400°C is not expected. It is important to note that these preliminary investigations on possible reactions between Zircaloy and Zn4Al need to be confirmed through an investigation of interfacial regions.

Figure 8. Castings of Zn-Al eutectic within MgO crucibles in the furnace.

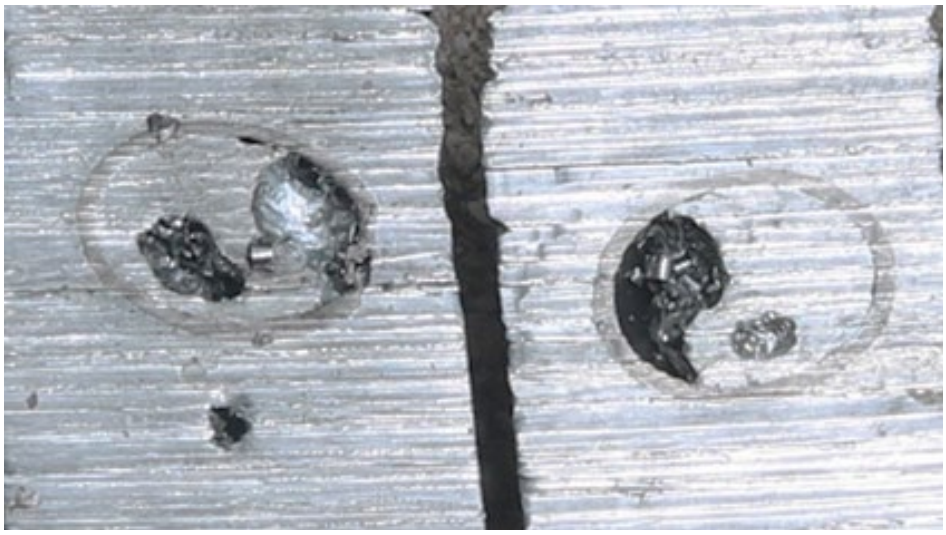

Figure 9. As-cut cross sections through casting with Zircaloy tube. The void within the tube was mainly due to the filling pattern and air entrapment after tube rotation.

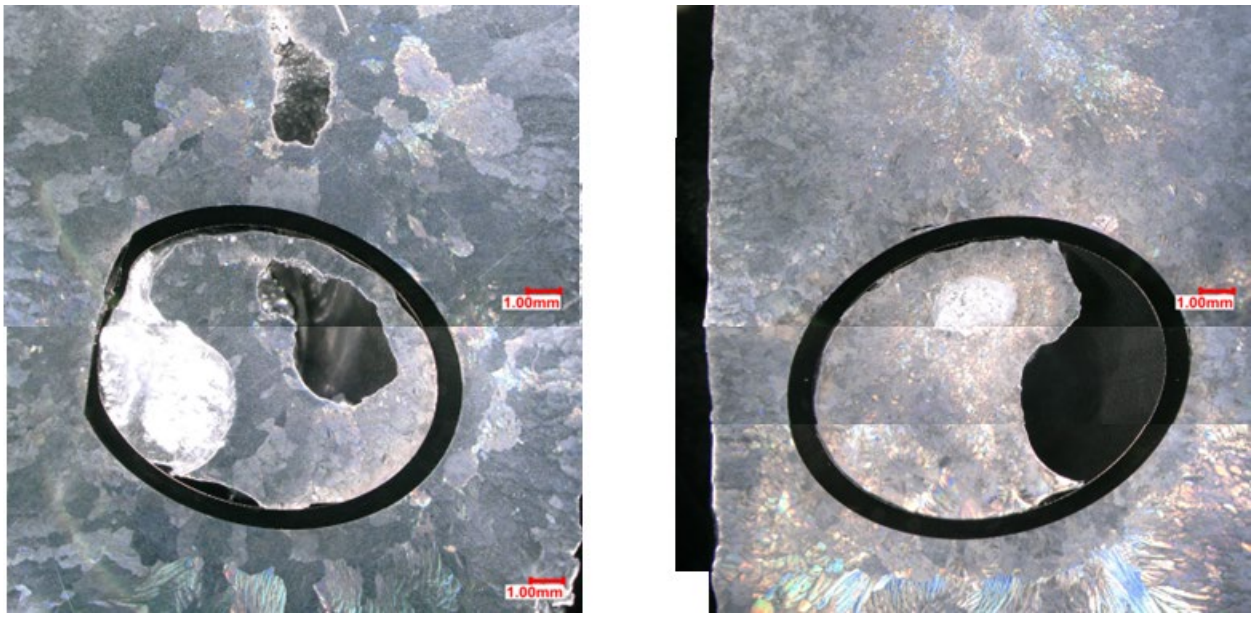

Figure 10. Polished cross sections of the specimens from Figure 9. The dark ring is the Zircaloy tube.

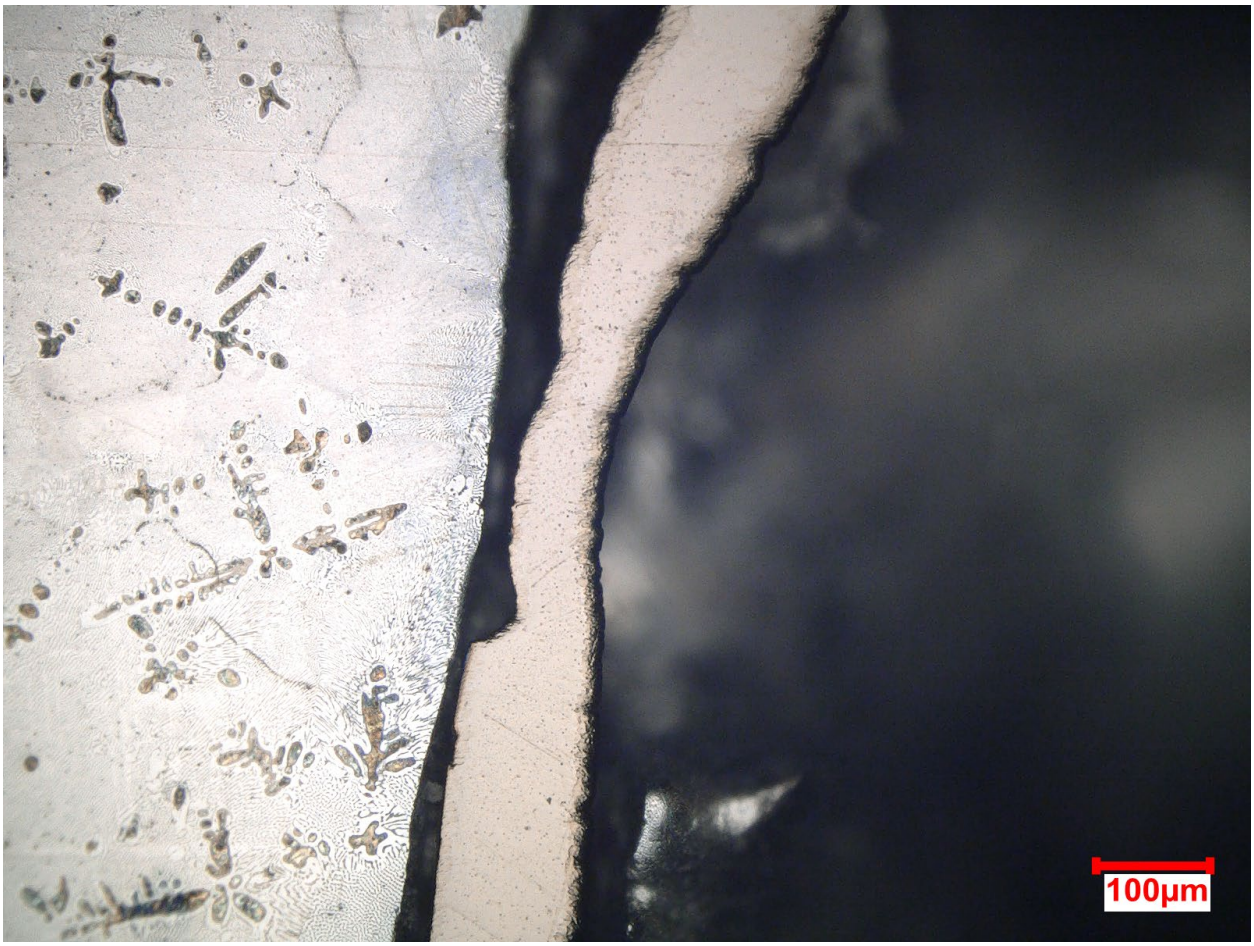

Figure 11. Ring zone (as polished 20 x +) near the tube end using coaxial lighting.

5. CONCLUSION

In FY 23, metallic remedial fillers for direct DPC disposal were studied to determine filling efficacy and materials compatibility and to review promising alloy filler candidates. Examination of a casting of a low-temperature Sn-Bi eutectic from FY 2022 found excellent filling and nearly complete inclusion within the mold. Preliminary interaction testing of Zn-Al eutectic with Zircaloy cladding material suggest little chemical interaction at relevant temperature. Separate tasks for a DPC filling facility concept report and the effect of DPC fillers on FEPs relevant to the disposal of SNF were reported by Fortner et al. (2023) and Price et al. (2023), respectively.

Planned future activities include:

- Further alloy melt interaction tests with Zircaloy, extending time in melt, and adding pre-oxidized Zircaloy. Other clad materials (e.g., M5) may be studied.
- Scale-up pour demonstration test, akin to that done in FY 22, using the Zn-Al alloy at higher temperature with more internal surfaces
- Corrosion testing of filler materials
- Further modeling of DPC pre-heating requirements, cooldown times, and cost estimates of filling
- Examine alternate filler materials (e.g., particulate glass)

6. REFERENCES

Alibabaie, S., Mahmudi, R., 2012. "Microstructure and creep characteristics of Zn–3Cu–xAl ultra high-temperature lead-free solders." *Mater. Des.* 39, 397–403. https://doi.org/10.1016/j.matdes.2012.03.005

ASTM, 2022. B86, Standard specification for zinc and zinc-aluminum (ZA) alloy foundry and die castings. https://doi.org/10.1520/B0086-22

Barnhurst, R.J., 1990. Zinc and Zinc Alloys. https://doi.org/10.31399/asm.hb.v02.a0001077

Cao, W., Chen, S.-L., Zhang, F., Wu, K., Yang, Y., Chang, Y.A., Schmid-Fetzer, R., Oates, W.A., 2009. "PANDAT software with PanEngine, PanOptimizer and PanPrecipitation for multi-component phase diagram calculation and materials property simulation." *Calphad, Tools for Computational Thermodynamics* 33, 328–342. https://doi.org/10.1016/j.calphad.2008.08.004

Chen, R.Y., Willis, D.J., 2005. "The behavior of silicon in the solidification of Zn-55Al-1.6Si coating on steel." *Metall. Mater. Trans. A* 36, 117–128. https://doi.org/10.1007/s11661-005-0144-x

Chen, T.J., Hao, Y., Sun, J., Li, Y.D., 2003. "Effects of Mg and RE additions on the semi-solid microstructure of a zinc alloy ZA27." *Sci. Technol. Adv. Mater.* 4, 495. https://doi.org/10.1016/j.stam.2004.01.002

Chen, Y.R., Zhang, F., 2020. "Pandat™ Simulation of the Solidification Sequence and Microstructure Development of the 2 Pct Mg-55 Pct Al-1.6 Pct Si-Zn Coating on Steel." *Metall. Mater. Trans. A* 51, 5228–5244. https://doi.org/10.1007/s11661-020-05936-5

Chuang, T.H., Tsao, L.C., Tsai, T.C., Yeh, M.S., Wu, C.S., 2000. "Development of a low-melting-point filler metal for brazing aluminum alloys." *Metall. Mater. Trans. A* 31, 2239–2245. https://doi.org/10.1007/s11661-000-0141-z

Clarity, J. B., et al. "As-Loaded Criticality Margin Assessment of Dual-Purpose Canisters Using UNF-ST&DARDS," *Nucl. Technol.*, vol. 199, no. 3, pp. 245–275, 2017.

Cumberland, R., et al., *Dual-Purpose Canister Filling Demonstration Performance Criteria Report*, ORNL/SPR-2022/2405 (March 31, 2022).

da Costa, E.M., da Costa, C.E., Vecchia, F.D., Rick, C., Scherer, M., dos Santos, C.A., Dedavid, B.A., 2009. "Study of the influence of copper and magnesium additions on the microstructure formation of Zn–Al hypoeutectic alloys." *J. Alloys Compd*. 488, 89–99. https://doi.org/10.1016/j.jallcom.2009.08.125

Dobosz, A. and Ganxarz, T. 2018. "Reference Data for the Density, Viscosity, and Surface Tension of Liquid Al-Zn, Ag-Sn, Bi-Sn, Cu-Sn, and Sn-Zn Eutectic Alloys." *J. Phys. Chem. Ref. Data* 47, 013102. doi: 10.1063/1.5010151.

DOE, 2004. "Clad Degradation – Summary and Abstraction for LA." ANL-WIS-MD-000021 REV 01, Bechtel SAIC, October 2004

Engin, S., Böyük, U., Kaya, H., Maraşlı, N., 2011. "Directional solidification and physical properties measurements of the zinc-aluminum eutectic alloy." *Int. J. Miner. Metall. Mater.* 18, 659–664. https://doi.org/10.1007/s12613-011-0492-z

Eqal, A.K., Yagoob, J.A., 2021. "Prediction of the solidification mechanism of ZA alloys using Ansys Fluent." *J. Appl. Sci. Eng*. 24, 699–706. https://doi.org/10.6180/jase.202110_24(5).0002

Fortner, J. A., et al., *Dual-Purpose Canister Filling Demonstration Project Progress Report*. ORNL/SPR-2022/2629 (September 30, 2022).

Fortner, J. A., et al., *Dual-Purpose Canister Filling Facility Concept Report*. ORNL/SPR-2023/2921 (May 31, 2023).

Gold, R. E., et al., "Evaluation of Zinc Addition to the Primary Coolant of PWRs." WESTINGHOUSE ELECTRIC CORPORATION Nuclear Services Division, TR-106358-V2 4023-01 (August 1996).

Goodwin, F., 2013. Development of Thin Section Zinc Die Casting Technology. Advanced Technology Inst., Norfolk, VA (United States). https://doi.org/10.2172/1111101

Guo, J., Samonds, M.T., 2007. "Alloy Thermal Physical Property Prediction Coupled Computational Thermodynamics with Back Diffusion Consideration." *J. Phase Equilibria Diffus*. 28, 58–63. https://doi.org/10.1007/s11669-006-9005-6

Guo, J., Samonds, M.T., 2004. "Property prediction with coupled macro-micromodeling and computational thermodynamics," in MCSP6-2004, MCSP6-2004. Presented at The 6th Pacific Rim International Conference on Modeling of Casting and Solidification Processes, Kaohsiung, Taiwan, pp. 157–164.

Hardin, E. et al., 2014. *Investigations of Dual-Purpose Canister Direct Disposal Feasibility (FY14).* FCRD-UFD-2014-000069. Albuquerque: Sandia National Laboratories. https://www.energy.gov/sites/prod/files/2014/10/f19/7FCRDUFD2014000069R1%20DPC%20DirectDispFeasibility.pdf

Hasan, M. M., Sharif, A., Gafur, M.A., 2020a. "Effect of Minor Addition of Ni on the Microstructure and Properties of Zn-Based High-Temperature Solder." *J. Electron. Mater*. 49, 3990–4001. https://doi.org/10.1007/s11664-020-08089-8

Hasan, Mohammad Mehedi, Sharif, A., Gafur, M.A., 2020b. "Characteristics of eutectic and near-eutectic Zn–Al alloys as high-temperature lead-free solders." *J. Mater. Sci. Mater. Electron.* 31, 1691–1702. https://doi.org/10.1007/s10854-019-02687-x

Jubin, R.T., Banerjee, K., Severynse, T.F., 2015. "Evaluation of Filler Materials to Control Post-Closure Criticality of Dual-Purpose Canisters." Presented at the 15th International High-Level Radioactive Waste Management Conference (IHLRWM 2015), Oak Ridge National Laboratory (ORNL), Oak Ridge, TN (United States), Charleston, SC, USA.

Kim, S.-J., et al., 2008. "Characteristics of Zn-Al-Cu Alloys for High Temperature Solder Application." *Mater. Trans*. 49, 1531–1536. https://doi.org/10.2320/matertrans.MF200809

Li, H., Li, Z., Liu, Y., Jiang, H., 2014. "Effect of zirconium on the microstructure and mechanical properties of Zn–4%Al hypoeutectic alloy." *J. Alloys Compd*. 592, 127–134. https://doi.org/10.1016/j.jallcom.2013.12.133

Liang, S.-M., Wu, Z., Sandlöbes, S., Korte-Kerzel, S., Schmid-Fetzer, R., 2019. "Analysis of microstructure formation in cast Zn alloys derived from computational thermodynamics of the Zn–Al–Cu–Mg system." *J. Mater. Sci.* 54, 9887–9906. https://doi.org/10.1007/s10853-019-03553-1

Liu, Y.H., 2006. "Density and viscosity of molten Zn-Al alloys." *Metall. Mater. Trans*. A 37, 2767–2771. https://doi.org/10.1007/BF02586109

Maheras, S. J., Best, R., Ross, S. B., Lahti, E. A., Richmond, D. J., 2012. *A Preliminary Evaluation of Using Fill Materials to Stabilize Used Nuclear Fuel During Storage and Transportation* (No. PNNL-21664). Pacific Northwest National Laboratory (PNNL), Richland, WA (United States). https://doi.org/10.2172/1052524

Meschel, S.V., Kleppa, O.J., 1993. "Standard enthalpies of formation of 4d aluminides by direct synthesis calorimetry." *J. Alloys Compd.* 191, 111–116. https://doi.org/10.1016/0925-8388(93)90280-Z

Park, Y., McKrell, T.J., Driscoll, M.J., 2017. "Heat transfer enhancement for spent nuclear fuel assembly disposal packages using metallic void fillers: A prevention technique for solidification shrinkage-induced interfacial gaps." *J. Nucl. Mater*. 489, 196–202. https://doi.org/10.1016/j.jnucmat.2017.04.001

Peng, C., Zhu, D., Li, K., Du, X., Zhao, F., Wan, M., Tan, Y., 2021. "Research on a Low Melting Point Al-Si-Cu (Ni) Filler Metal for 6063 Aluminum Alloy Brazing." *Appl. Sci.* 11, 4296. https://doi.org/10.3390/app11094296

Petzow, G., 1991. *Ternary alloys A comprehensive compendium of evaluated constitutional data and phase diagrams*, Vol 4. VCH Verlagsges, Germany.

Pola, A., Roberti, R., Montesano, L., 2010. "New Zinc alloys for semisolid applications." *Int. J. Mater. Form.* 3, 743–746. https://doi.org/10.1007/s12289-010-0877-y

Price, L., et al., 2023, "The Effect of DPC Fillers on FEPs Relevant to Disposal of SNF," M3SF-23SN010305093 August 31, 2023.

Puig, F., Dies, J., Pablo, J. de, Martínez-Esparza, A., 2008. "Spent fuel canister for geological repository: Inner material requirements and candidates evaluation." *J. Nucl. Mater.* 376, 181–191. https://doi.org/10.1016/j.jnucmat.2008.02.069

Risueño, E., Faik, A., Gil, A., Rodríguez-Aseguinolaza, J., Tello, M., D'Aguanno, B., 2017. "Zinc-rich eutectic alloys for high energy density latent heat storage applications." *J. Alloys Compd*. 705, 714–721. https://doi.org/10.1016/j.jallcom.2017.02.173

Risueño, E., Faik, A., Rodríguez-Aseguinolaza, J., Blanco-Rodríguez, P., Gil, A., Tello, M., D'Aguanno, B., 2015. "Mg-Zn-Al Eutectic Alloys as Phase Change Material for Latent Heat Thermal Energy Storage." Int. Conf. Conc. Sol. Power Chem. Energy Syst. *SolarPACES* 2014 69, 1006–1013. https://doi.org/10.1016/j.egypro.2015.03.193

Sadayappan, K., Elsayed, A., 2018. Sand Casting of Aluminum Alloys. https://doi.org/10.31399/asm.hb.v02a.a0006533

Schaefer, R. J., et al., *Interaction of Zinc Vapor with Zircaloy and the Effect of Zinc Vapor on the Mechanical Properties of Zircaloy*. NIST NUREG/CR-6675 (June 2000).

Sigworth, G., 2018. Solidification and Castability of Foundry Alloys. https://doi.org/10.31399/asm.hb.v02a.a0006496

Tsao, L.C., Chiang, M. J., Lin, W. H., Cheng, M. D., Chuang, T. H., 2002. "Effects of zinc additions on the microstructure and melting temperatures of Al–Si–Cu filler metals." *Mater. Charact.* 48, 341–346. https://doi.org/10.1016/S1044-5803(02)00276-0

Türk, A., Durman, M., Kayali, E.S., 2007. "The effect of manganese on the microstructure and mechanical properties of zinc–aluminium based ZA-8 alloy." *J. Mater. Sci. 42*, 8298–8305. https://doi.org/10.1007/s10853-007-1504-2

Williams, M., "The Reactions of Zinc Vapor with ZIRCALOY-4 and Pure Zirconium." NIST NISTIR 6447 (January 2000).